

# Optical response of two-dimensional electron fluids beyond the Kohn regime: strong non-parabolic confinement and intense laser light

M. Santer,<sup>1</sup> B. Mehlig,<sup>2</sup> and M. Moseler<sup>1</sup>

<sup>1</sup>*Theoretical Quantum Dynamics, University of Freiburg, 79104 Freiburg, Germany*

<sup>2</sup>*School of Physics and Engineering Physics, Gothenburg University/Chalmers, 412 96 Gothenburg, Sweden*

We investigate the linear and non-linear optical response of two-dimensional (2D) interacting electron fluids confined by a strong non-parabolic potential. We show that such fluids may exhibit higher-harmonic spectra under realistic experimental conditions. Higher harmonics arise as the electrons explore anharmonicities of the confinement potential (electron-electron interactions reduce this non-linear effect). This opens the possibility of controlling the optical functionality of such systems by engineering the confinement potential. Our results were obtained within time-dependent density-functional theory, employing the adiabatic local-density approximation. A classical hydrodynamical model is in good agreement with the quantum-mechanical results.

Confined, two-dimensional (2D) electronic quantum systems have been subject to intense theoretical and experimental investigations during the last two decades<sup>1</sup>. Emerging from quantum-well structures or charge layers in modulation doped semiconductor interfaces, they are nowadays routinely tailored into quantum dots<sup>2,3</sup> or strips<sup>4</sup>. Possible applications range from single-electron transistors to coherent, tunable light sources for far-infrared (FIR) spectroscopy<sup>5</sup>, a method which has proven a powerful tool for probing slow vibrational modes in molecular and condensed matter systems. In the light of this application and in order to design future 2D THz devices, a detailed understanding of linear – and non-linear – excitation mechanisms in confined 2D electronic quantum systems is necessary.

In finite 2D systems (such as, e.g., quantum dots or quantum strips), the linear optical response depends on the shape of the confinement potential  $v_0$ . Recent experimental results concern parabolic or near-parabolic confinement potentials<sup>2</sup> for which the so-called harmonic potential theorem (HPT) states that an external dipole excitation can only couple to a rigid-shift mode (Kohn mode<sup>6</sup>) at frequency  $\sqrt{K/m^*}$  independently of the excitation strength<sup>7</sup> ( $m^*$  is the effective electron mass and  $K$  the curvature of  $v_0$ ). In its original formulation, the HPT is a quantum-mechanical theorem<sup>7,8</sup>; it was shown<sup>9</sup> to hold in classical mechanics also.

In realistic, finite 2D quantum structures, the confinement potential  $v_0$  is often strongly modulated (e.g. by inhomogeneous charge distributions) exhibiting a pronounced anharmonicity<sup>10</sup>. Nevertheless, in many experiments, the Kohn mode dominates the response<sup>11</sup>. This is because for weak external fields, and for low electron densities, anharmonic regions of the confinement potential are hardly explored. Experimentally it is possible to overcome the HPT limitations in at least two ways: either by increasing the density  $\bar{n}$  of conduction electrons or by increasing the intensity of the laser light. This makes it possible to experimentally investigate the hydrodynamics of the interacting electron fluid, which is expected to reveal much more information about the electron dynamics than the rigid-shift response in the Kohn regime.

However, in order to adequately describe the case of strong fields, the non-linear response of the conduction electrons must be considered. While the non-linear response of atoms<sup>12,13</sup>, molecules<sup>14,15</sup>, nanotubes<sup>16,17</sup>, and 3D quantum dots<sup>18,19</sup> has been thoroughly investigated, little is known about the non-linear response of finite, interacting 2D electronic systems to intense laser fields. Is it possible to observe higher-harmonic (HH) generation, either due to anharmonicities in the confinement potential, or as a consequence of nonlinearities in the hydrodynamics of the conduction electrons? Do existing THz sources (such as free-electron lasers) provide sufficient intensity to observe HH generation in such systems?

Alternatively, one may consider weak fields (linear regime), but high conduction-electron densities. However, most theoretical studies of the linear response either consider the case of low densities of conduction electrons where the confinement potential can be assumed to be parabolic<sup>20</sup>, or the other extreme, “classical” confinement by infinitely high potential barriers<sup>21</sup>. How the nature of the optical response changes in realistic systems as the density of conduction electrons is increased (so that they explore more and more of the anharmonic parts of the confinement potential  $v_0$ ) is not known. How does the Kohn mode compete with other modes of excitation when the HPT is no longer valid?

Last but not least, to which extent can a classical model<sup>22</sup> of the (non-)linear response be adequate in a regime beyond the HPT? Such a model would have to account for the hydrodynamics of the electron fluid. In the present article we address the above questions within a classical hydrodynamic model, and within a quantum-mechanical approach, time-dependent density-functional theory<sup>23</sup> (TDDFT).

*Model.* Our model is described in Fig. 1. We assume that the confinement potential  $v_0$  is supplied by a 2D rigid positive jellium charge. If neutralised with charge carriers this model corresponds to a 2D metallic strip<sup>24</sup>. It can be regarded as a model of modulation-doped semiconductor heterostructures embedded in a dielectric medium where a layer of dopant charges corresponds to the positive background. How these, in combi-

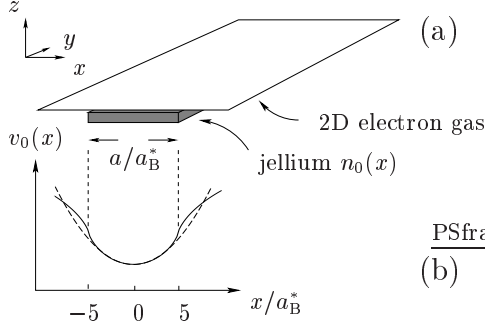


FIG. 1: (a) Schematic representation of the system considered, a 2D electron gas in the  $x$ - $y$ -plane, confined further in the  $x$ -direction by a positively charged (charge density  $n_0$ ) rigid jellium strip oriented along the  $y$ -axis, of width  $a$ . A filling fraction is defined by  $\eta = \bar{n}/n_0$ . (b) Electrostatic potential  $v_0(x)$  [arb. un.] of the jellium charge (solid line) for  $a = 10a_B^*$  and  $r_0 \approx 0.47$  [a.u.]. Reduced atomic units are used throughout,  $a_B^*$  is the reduced Bohr radius. Around  $x=0$ , the confinement potential is harmonic,  $v_0(x) \approx (K/2)x^2$  (dashed line) with  $K = 8n_0/a$ . For large values of  $x$  ( $|x| > a/2$ ),  $v_0$  grows logarithmically.

nation with vertical gate voltages, can modify the overall confinement potential is discussed in Ref. 10.

In the following we show results for two cases, wide and narrow confinement in the  $x$ -direction ( $a = 100a_B^*$  and  $10a_B^*$ , respectively); corresponding to very shallow confinement in the case of  $a = 100a_B^*$ , and very strong confinement for  $a = 10a_B^*$ . In GaAs, the widths correspond to roughly  $1\mu\text{m}$  and  $100\text{nm}$ , respectively. The filling fraction  $\eta$  is a parameter ( $0 \leq \eta \leq 1$ ). For a given value of  $\eta$ , the electron charge per unit length (in the  $y$ -direction) is taken to be the same in both cases. The system is subjected to an electric field  $\mathbf{E}(t) = E_x(t)\hat{\mathbf{e}}_x$  pointing in the  $x$ -direction,  $\hat{\mathbf{e}}_x$ .

*Methods.* Due to translational symmetry in the  $y$ -direction, the problem reduces to a one-dimensional self-consistent one, of determining the dynamics of the electronic density profile  $n(x, t)$  in the potential

$$v([n]; x, t) = xE_x(t) + v_{\text{xc}}([n]; x, t) + 2 \int dx' [n(x', t) - n_0(x')] \log |x - x'|. \quad (1)$$

Our quantum-mechanical solution<sup>33</sup> to this problem relies on the TDDFT<sup>23</sup>, the exchange-correlation potential  $v_{\text{xc}}([n]; x, t)$  was treated in the adiabatic local-density approximation (ALDA)<sup>25</sup>. The quantum-mechanical wave-packet dynamics was started from the ground state of the unperturbed system (with  $E_x = 0$ ), i. e., the solution of the static Kohn-Sham equations<sup>26</sup>.

We have compared our TDDFT results with a classical approach: the classical hydrodynamics of the electron fluid (neglecting  $v_{\text{xc}}$ ) was solved in a co-moving Lagrange frame<sup>27</sup>, represented by a layer of infinitely thin rods of width  $dx$  with initial positions  $x$ , infinitesimal charges  $n(x, 0)dx$  (per unit-length), and velocities  $u(x, t)$ , evolv-

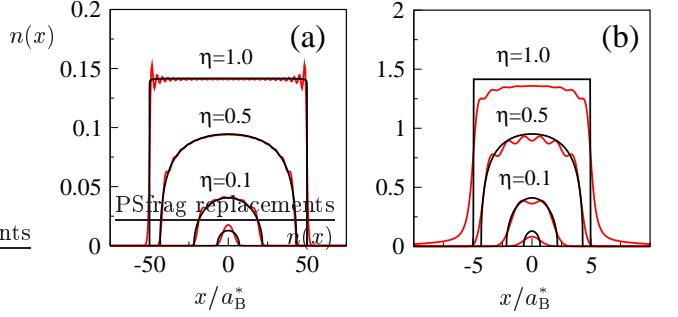


FIG. 2: (a) Classical (black lines) and quantum-mechanical (red lines) ground-state charge-density distributions for  $a = 100a_B^*$ , for different values of the parameter  $\eta$  (charging fraction), from  $\eta = 0.01$  to  $\eta = 1$ . (b) Same, but for  $a = 10a_B^*$ .

ing according to Newton's law  $\partial_t u(x, t) = -\partial_x v([n]; x, t)$ . The classical wave-packet dynamics was started from the stationary solution  $n(x)$  of  $\partial_x v([n]; x, 0) = 0$ . It was found by relaxing an initial Gaussian density profile with additional, suitably chosen Stokes damping. Since the static screening length of a 2D electron gas is considerably larger than the inter-particle distance, this classical hydrodynamical approach is expected to work well. It neglects exchange, correlation, and shell effects.

*Ground-state properties.* Classical and quantum-mechanical ground-state density profiles are shown in Fig. 2. For the wide system, the agreement between classical and quantum-mechanical profiles is satisfactory for most values of  $\eta$ , except for large  $\eta$  (where the quantum-mechanical profile exhibits Friedel oscillations), and for small values of  $\eta$  (where the quantum-mechanical profile is Gaussian while the classical one is elliptic). In the narrow system, the discrepancies are larger. For large  $\eta$ , electron spill-out dominates the quantum-mechanical profile.

*Linear response.* The linear response is obtained by applying a low-intensity white-light pulse  $E_x(t) = E_0 \delta(t)$ . A value of  $E_0 = 0.001$  [a.u.] was verified to be sufficiently small to remain within the regime of linear response, for the parameters considered here. We have calculated the dipolar strength function  $S(\omega) = (2\omega/E_0\pi)\text{Im } d(\omega)$ . Here  $d(\omega)$  is the Fourier transform of the dipole moment.

In Figs. 3(a) and (b) our results for  $S(\omega)$  are shown. For low conduction-electron densities ( $\eta = 0.1$ ), nearly all dipolar strength is in the Kohn mode for both the wide and the narrow system, as expected. The classical and quantum-mechanical strength functions are almost indistinguishable [insets of Figs. 3(a) and (b)]. As the filling fraction is increased, higher plasmon modes develop in the case of the wide system [Fig. 3(a)]. Classical and quantum-mechanical results agree fairly well, except for large values of  $\omega$  where the classical plasmon dispersion is found to underestimate the quantum-mechanical result. The results for the narrow system at  $\eta = 1$  are very different [Fig. 3(b)]: here we observe strong Landau fragmentation<sup>28</sup> of the main peak; all higher-order

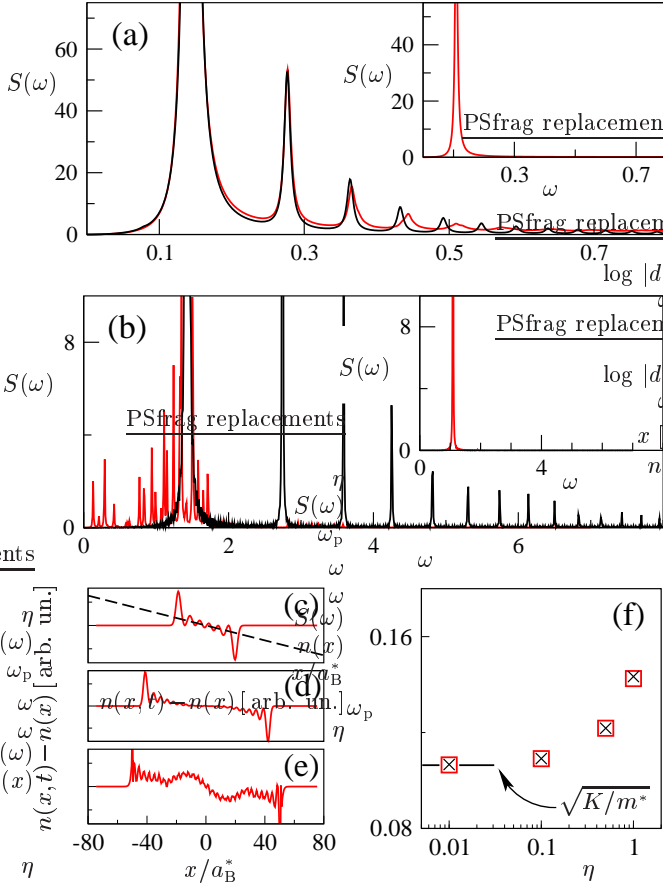


FIG. 3: (a) Quantum-mechanical (red lines) and classical (black lines) linear response for  $a = 100 a_B^*$  and  $\eta = 1$ . Inset: same, but for  $\eta = 0.1$ . (b) Same, but for  $a = 10 a_B^*$  and  $\eta = 0.1, 1$ . (c-e) Snapshots of density profiles for  $a = 100 a_B^*$  and  $\eta = 0.1, 0.5$  and  $1$ . For  $\eta = 0.1$ , the profile is dominated by the Kohn mode (dashed line). (f) Position of the first plasmon resonance as a function of  $\eta$  for  $a = 100 a_B^*$ . Shown are classical ( $\times$ ) and quantum-mechanical results ( $\square$ ).

plasmon modes disappear. The classical approximation is inadequate in this regime.

What is the spatial profile of the modes observed in Figs. 3(a) and (b)? The Kohn mode (small  $\eta$ ) is a rigid-shift mode. As  $\eta$  approaches unity in the wide system, it evolves into the first plasmon mode, a combination of a rigid-shift and a hydrodynamic mode (the higher modes are expected to be hydrodynamic modes for all values of  $\eta$ ). These two modes of oscillation correspond to Goldhaber-Teller and Steinwedel-Jensen modes in atomic nuclei<sup>29</sup>. Figs. 3(c-e) show snapshots of quantum-mechanical density profiles for three values of  $\eta$  in the wide system. By virtue of selection rules,  $n(x, t) - n(x)$  is antisymmetric w.r.t. reflection at  $x = 0$ . For small  $\eta$ , the rigid-shift mode dominates and  $n(x, t) - n(x) \propto -x$  near the origin (note that the rigid-shift profile has the time-dependence  $n(x, t) = n(x - x_{cm}(t), 0)$  where  $x_{cm}$  is the center-of-mass of the profile). As  $\eta$  increases, hydrodynamic modes emerge. They correspond, approxi-

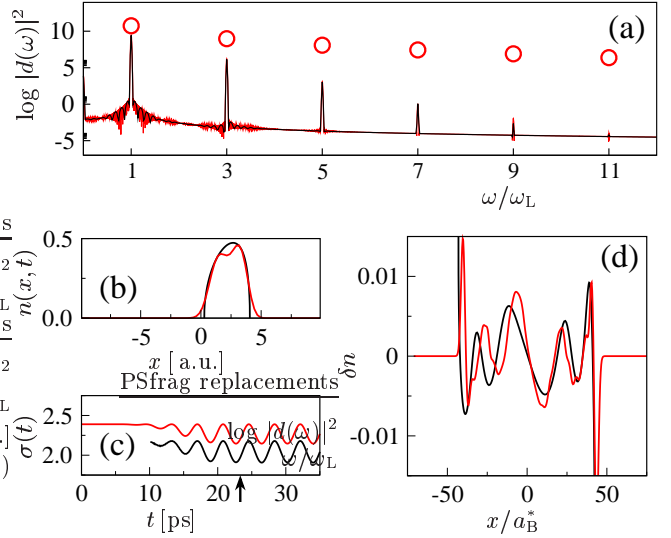


FIG. 4: (a) Non-linear response for  $a = 10 a_B^*$ ,  $\omega_L = 0.05$  [a.u.] (0.13 THz),  $\eta = 0.1$ , and  $E_0 = 3$  [a.u.] (intensity  $1.38 \cdot 10^6$  W/cm $^2$ ). Shown are classical (black lines), TDDFT results (red lines), and quantum-mechanical independent-particle results (circles). (b) Density profile for the same parameters as in (a), but  $E_0 = 1$  [a.u.] at  $t = 22.8$  ps. (c) Time evolution of the width  $\sigma$  of this density profile (the arrow indicates  $t = 22.8$  ps). (d)  $\delta n \equiv n(x - x_{cm}(t), t) - n(x)$  for  $a = 100 a_B^*$ ,  $\omega_L = 0.45$  [a.u.],  $\eta = 0.5$ , and  $E_0 = 0.5$  [a.u.] (intensity  $3.8 \cdot 10^4$  W/cm $^2$ ),  $t = 4.5$  ps.

mately, to standing waves (reflected at  $\pm a/2$ ) with wave vectors  $q = \pi\nu/a$  with  $\nu = 0, 1, \dots$  and frequencies  $\omega_p^2(q) = 2\pi n_0/(\varepsilon m^*) q$  ( $\varepsilon$  is the dielectric constant). Here  $\omega_p^2(q)$  is the plasmon dispersion for a spatially extended 2D electron fluid, the confinement is modeled by assuming that the wave-length corresponding to  $q$  is given by the width  $a$ . Fig. 3(f) shows how the position of the first ( $\nu = 1$ ) plasmon resonance evolves as a function of  $\eta$ . For small  $\eta$ , the Kohn limit is reached, as expected. As  $\eta$  is increased, the position evolves, albeit not quite to the value  $\omega_p^2(q=2\pi/a) = 2\pi^2 n_0/(a\varepsilon m^*)$ . This is due to the fact that at  $\eta = 1$ , the profile of the density oscillations is not quite sinusoidal (see also Ref. 21): sinusoidal modes do not diagonalise the problem, their interaction gives rise to a frequency shift.

*Non-linear response.* The system was subjected to an intense monochromatic light wave of amplitude  $E_0$  and frequency  $\omega_L$  (switched on slowly, on the time scale of a few cycles). The laser intensities were chosen so as to avoid ionisation of the system, not exceeding  $10^6$  W/cm $^2$  (well within the range of standard free-electron lasers).

Fig. 4(a) shows classical and quantum-mechanical results for the dipolar power spectrum  $|d(\omega)|^2$  (see Ref. 30) in the narrow system. We observe excellent agreement between classical and quantum-mechanical results. Further, we observe HH at odd multiples of  $\omega_L$ . These HH are due to the electrons exploring the anharmonic potential  $v_0$  (c.f. scattering of electrons off the Coulomb

potential in ionised atoms). The parameters ( $\eta = 0.1$  and  $\omega_L = 0.05$  [a.u.]) were chosen to allow for large excursions of  $n(x, t)$  into the anharmonic regions of  $v_0$ .

Our observations show that confined, interacting 2D electron fluids do exhibit HH spectra, albeit not as prominently as in single-electron systems such as atoms in strong laser fields<sup>13</sup>. We surmise that the hydrodynamic modes arising from the nonlinearities in the fluid dynamics dampen the center-of-mass motion and its acceleration, reducing the intensity of HH. We have verified that a substantial center-of-mass acceleration is observed when the non-linear electron-electron interactions are switched off during the laser pulse, resulting in HH of considerably larger strength [Fig. 4(a)]. This implies that independent-electron models of 2D interacting electron fluids are likely to overestimate the strength of the non-linear response. Note that our quantum-mechanical results are not sensitive to the presence/absence of the exchange-correlation potential, indicating that  $v_{xc}$  has little influence on HH generation.

Following the strong external driving, the density profile  $n(x, t)$  moves with the frequency  $\omega_L$ , but not rigidly: in the narrow system, the width of the profile changes periodically (breathing mode), as shown in Figs. 4(b) and (c). This mode dampens the rigid-shift motion of the electron fluid (c.f. Ref. 31 for a similar effect in a circular, anharmonic quantum dot).

In the wide system (at  $\eta = 0.5$ ), electron-electron in-

teractions give rise to small-amplitude oscillations added to the otherwise rigidly moving density profile [Fig. 4(d)]. The time-dependence of the center-of-mass motion is found to be in good agreement with the classical model. In the small-amplitude oscillations, by contrast, a phase shift is observed<sup>34</sup>. Finally we emphasise that the selection rules of the linear case no longer hold [Fig. 4(d)].

*Conclusions.* We have analysed the linear and non-linear response of confined 2D, interacting electron fluids to laser light. Our results may be summarised as follows: First, non-parabolically confined interacting 2D electron fluids may exhibit HH spectra under realistic experimental conditions. HH are due to the electron fluid exploring anharmonicities in the confinement potential. It is found that electron-electron interactions dampen this effect. Second, with the exception of small systems at high electron densities (where single-particle excitations interact with the collective modes giving rise to considerable Landau fragmentation of the plasmons), a non-linear classical hydrodynamical model provides a very good approximation to the linear and non-linear response obtained within the TDDFT; exchange-correlation effects have a negligible influence. It would be of interest to ascertain to which extent the non-linear response of geometrically more complex systems such as nanotubes, quantum rings, clusters, or  $C_{60}$  can be modelled by the classical approach used here.

---

<sup>1</sup> T. Ando, A. Fowler, and F. Stern, Rev. Mod. Phys. **54**, 437 (1982).

<sup>2</sup> L. P. Kouwenhoven, D. G. Austing, and S. Tarucha, Rep. Prog. Phys. **64**, 701 (2001).

<sup>3</sup> Y. Alhassid, Rev. Mod. Phys. **72**, 895 (2000).

<sup>4</sup> T. Egeler et al., Phys. Rev. Lett. **65**, 1804 (1990).

<sup>5</sup> M. Vossebarger et al., J. Opt. Soc. Am. B **13**, 1045 (1996).

<sup>6</sup> W. Kohn, Phys. Rev. **123**, 1242 (1961).

<sup>7</sup> J. F. Dobson, Phys. Rev. Lett. **73**, 2244 (1994).

<sup>8</sup> S. K. Yip, Phys. Rev. B **43**, 1707 (1991).

<sup>9</sup> W. L. Schaich, M. R. Geller, and G. Vignale, Phys. Rev. B **53**, 13016 (1996).

<sup>10</sup> K. Lier and R. R. Gerhardts, Phys. Rev. B **48**, 14416 (1993).

<sup>11</sup> T. Demel, P. Heitmann, P. Grambow, and K. Ploog, Phys. Rev. Lett. **64**, 788 (1990).

<sup>12</sup> X. Chu and S.-I. Chu, Phys. Rev. A **63**, 023411 (2001).

<sup>13</sup> A. L'Huillier, L. A. Lompre, G. Mainfray, and C. Manus, in *Advances in atomic, molecular, and optical physics*, edited by M. Gavrila (Academic (New York), 1992), Supp. 1.

<sup>14</sup> F. Calvayrac et al., Phys. Rev. B **52**, R17056 (1995).

<sup>15</sup> S. J. A. van Gisbergen, J. G. Snijders, and E. J. Baerends, Phys. Rev. Lett. **78**, 3097 (1997).

<sup>16</sup> C. Stanciu et al., preprint (2002).

<sup>17</sup> O. E. Alon, V. Averbukh, and N. Moiseyev, Phys. Rev. Lett. **85**, 5218 (2000).

<sup>18</sup> N. H. Bonadeo et al., phys. stat. sol. (b) **221**, 5 (2000).

<sup>19</sup> L. Jönsson and G. Wendin, J. Opt. Soc. Am. B **9**, 627 (1992).

<sup>20</sup> L. Brey, J. Dempsey, N. F. Johnson, and B. I. Halperin, Phys. Rev. B **42**, 1240 (1990).

<sup>21</sup> W. L. Schaich and A. H. McDonald, Solid State Comm. **83**, 779 (1992).

<sup>22</sup> A. L. Fetter, Phys. Rev. B **33**, 5221 (1986).

<sup>23</sup> E. K. U. Gross, J. F. Dobson, and M. Petersilka, in *Topics in Current Chemistry*, edited by J. D. Dunitz et al. (1990), vol. 181, pp. 81–171.

<sup>24</sup> M. Santer and B. Mehlig, Phys. Rev. B **63**, art. no. 241403 (2001).

<sup>25</sup> K. Yabana and G. F. Bertsch, Phys. Rev. B **54**, 4484 (1996).

<sup>26</sup> W. Kohn and L. J. Sham, Phys. Rev. **140**, 1133 (1965).

<sup>27</sup> See Ref. 36 in: M. Moseler and U. Landman, Science **289**, 1165 (2000).

<sup>28</sup> M. Brack, Rev. Mod. Phys. **64**, 677 (1993).

<sup>29</sup> W. D. Myers, Phys. Rev. C **15**, 2032 (1977).

<sup>30</sup> F. Calvayrac, P. G. Reinhard, E. Suraud, and C. A. Ullrich, Phys. Rep. **337**, 493 (2000).

<sup>31</sup> A. Puente, L. Serra, and V. Gudmundsson, Phys. Rev. B **64**, 235324 (2001).

<sup>32</sup> B. Tanatar and D. M. Ceperley, Phys. Rev. B **39**, 5005 (1989).

<sup>33</sup> Within the TDDFT, the dynamics is determined by the time-dependent Kohn-Sham equations<sup>23</sup>. They were solved numerically using a split-operator technique<sup>30</sup>, a 6th-order finite-difference approximation of the kinetic energy operator and a 13th-order Taylor expansion of the propagator.

<sup>34</sup> The phase shift is found to increase to  $\pi$  as  $t$  increases.